FEBS Letters 583 (2009) 890–896

FEBS Letters

journal homepage: www.FEBSLetters.org

Biophysical characterization of a new *SCN5A* mutation S1333Y in a SIDS infant linked to long QT syndrome

Hai Huang [a], Gilles Millat [b], Claire Rodriguez-Lafrasse [b], Robert Rousson [b], Béatrice Kugener [c], Philippe Chevalier [d], Mohamed Chahine [a,e,*]

[a] Le Centre de Recherche Université Laval Robert-Giffard, Local F-6539, 2601 Chemin de la Canardière, Québec City, QC, Canada G1J 2G3
[b] Laboratoire de Biochimie et Biologie Moléculaire, Hôpital Cardiovasculaire et Pneumologique L Pradel, F-69677 Bron Cedex, France
[c] Unité de Neuro-pédiatrie, Hôpital Debrousse, Lyon, France
[d] Unité de Cardiologie et Soins Intensifs, Hôpital Cardiovasculaire et Pneumologique L Pradel, F-69677 Bron Cedex, France
[e] Departement de Médecine, Université Laval, Québec City, QC, Canada G1K 7P4

ARTICLE INFO

Article history:
Received 12 January 2009
Revised 3 February 2009
Accepted 4 February 2009
Available online 10 February 2009

Edited by Maurice Montal

Keywords:
Sudden infant death syndrome
Genetics
Na^+ channel
$Na_v1.5$
Long QT syndrome
SCN5A

ABSTRACT

Various entities and genetic etiologies, including inherited long QT syndrome type 3 (LQT3), contribute to sudden infant death syndrome (SIDS). The goal of our research was to biophysically characterize a new *SCN5A* mutation (S1333Y) in a SIDS infant. S1333Y channels showed the gain of Na^+ channel function characteristic of LQT3, including a persistent inward Na^+ current and an enhanced window current that was generated by a −8 mV shift in activation and a +7 mV shift in inactivation. The correlation between the biophysical data and arrhythmia susceptibility suggested that the SIDS was secondary to the LQT3-associated S1333Y mutation.

1. Introduction

The most common cause of mortality during the first year of life of infants in developed countries is sudden infant death syndrome (SIDS), which is more common in infants placed in a prone position [1] or with upper respiratory infections [2]. Other risk factors include bottle feeding, second-hand smoke, overheating, and co-sleeping [3]. Previous studies revealed that SIDS is associated with alterations in genes associated with cardiac ion channels, including human cardiac voltage-gated Na^+ channels ($Na_v1.5$) [4].

Inherited long QT syndrome (LQTS) accounts for about 9.5% of SIDS cases, suggesting that sudden death due to cardiac arrhythmias is an important contributor to SIDS [5]. LQTS is caused by delayed ventricular repolarization, which leads to fatal ventricular arrhythmias and even sudden death. Inherited LQT3 linked to mutations in *SCN5A* has also been directly linked to SIDS [6–10]. *SCN5A* is the major gene known to functionally encode the α-subunit of the human cardiac voltage-gated Na^+ channel, which is responsible for the initiation and propagation of the cardiac action potential. The hallmark of the gating change in LQT3 mutations is the presence of persistent inward Na^+ currents due to incomplete inactivation or late re-opening of Na^+ channels, as a result, QT interval prolongation. Most LQT3 mutations are located in the III–IV linker, various domains of the S4–S5 linkers, voltage sensors, and the C-terminus of Na^+ channels, which are associated with the fast inactivation process. The S4–S5 linker of domain III plays a major role in the kinetics and voltage dependence of fast inactivation of Na^+ channels by acting as a docking site for the inactivation particle of the III–IV linker [11].

In this work we report a new SIDS mutation (S1333Y) in a 25-day-old infant, which is located in the S4–S5 linker of domain III [12], and we characterize its biophysical properties.

2. Methods

2.1. Clinical evaluation and molecular genetics

The local ethics committee approved the study protocol. The parents provided written informed consent. The death certificate indicated a diagnosis of SIDS, while the autopsy, toxicology, and review of the circumstances of death were negative. Genomic DNA

* Corresponding author. Address: Le Centre de Recherche Université Laval Robert-Giffard, Local F-6539, 2601 Chemin de la Canardière, Québec City, QC, Canada G1J 2G3. Fax: +1 418 663 8756.
E-mail address: mohamed.chahine@phc.ulaval.ca (M. Chahine).

0014-5793/$36.00
doi:10.1016/j.febslet.2009.02.007

was extracted from whole blood using a WIZARD Genomic DNA Purification kit (Promega, Madison, WI, USA). The coding exons of the *KCNQ1, KCNH2, SCN5A, KCNE1*, and *KCNE2* genes were amplified separately using intronic primers and previously reported PCR conditions [13]. Denaturing high performance liquid chromatography (DHPLC) was performed using previously described elution profiles and melting temperatures [12]. PCR products with divergent chromatographic profiles were directly sequenced on both strands using the BigDye® Terminator v.31 Cycle sequencing kit (Applied Biosystems, Forster City, CA, USA) and were applied to an ABI 3100 automatic sequencer.

2.2. Mutagenesis

Mutant hNa$_v$1.5/S1333Y was generated using a QuickChange TM site-directed mutagenesis kit according to the manufacturer's instructions (Stratagene, La Jolla, CA, USA). The oligo-nucleotide primers containing the corresponding S1333Y mutation were synthesized using the following sequences:

5′-GTG GGC GTC GCC ATC CCG TAC ATC ATG AAC GTC CTC-3′ (forward primer) and 5′-GAG GAC GAG GTT CAT GAT GTA CGG GAT GGC GCC CAC-3′ (reverse primer).

The mutated site is underlined. Mutant and WT Na$_v$1.5 channels were inserted in a pcDNA1 construct and were purified using Qiagen columns (Qiagen Inc., Chatsworth, CA, USA).

2.3. TsA201 transfection and patch clamp experiments

Mutant channels were coexpressed with the β subunit in the tsA201 human cell line and characterized using the patch clamp technique in whole-cell configuration as already reported [14].

2.4. Solutions and reagents

For the whole-cell recordings, the patch pipettes were filled with 35 mM NaCl, 105 mM CsF, 10 mM EGTA, and 10 mM Cs-HEPES. The pH was adjusted to 7.4 using 1 N CsOH. The bath solution contained 150 mM NaCl, 2 mM KCl, 1.5 mM $CaCl_2$, 1 mM $MgCl_2$, 10 mM glucose, and 10 mM Na-HEPES. The pH was adjusted to pH 7.4 using 1 N NaOH (final Na^+: 152.4 mM). The liquid junction potential between the patch pipette and the bath solution was corrected to −7 mV.

2.5. Statistical analysis

Results are presented as means ± standard errors of the mean. Statistical comparisons were made using the unpaired Student's *t*-test in SigmaStat (Jandel Scientific Software, San Rafael, CA, USA). Differences were considered significant at $P < 0.05$.

3. Results

3.1. Identification of the SCN5A mutation S1333Y

The genomic DNA of the SIDS infant was screened for sequence changes in all 28 exons of *SCN5A* by DHPLC analysis. The PCR analysis of the *SCN5A* gene revealed a mutation that was a compound heterozygote with *SCN5A*/S1333Y and *KCNE1*/T20I (Fig. 1A and B). The family members of the infant were screened clinically and genetically. *SCN5A*/S1333Y was a spontaneous mutation and the father was found to be the carrier of the *KCNE1*/T20I mutation with no LQTS-related phenotypes. Other family members were negative in the screen. It was hypothesized that the S1333Y mutation is

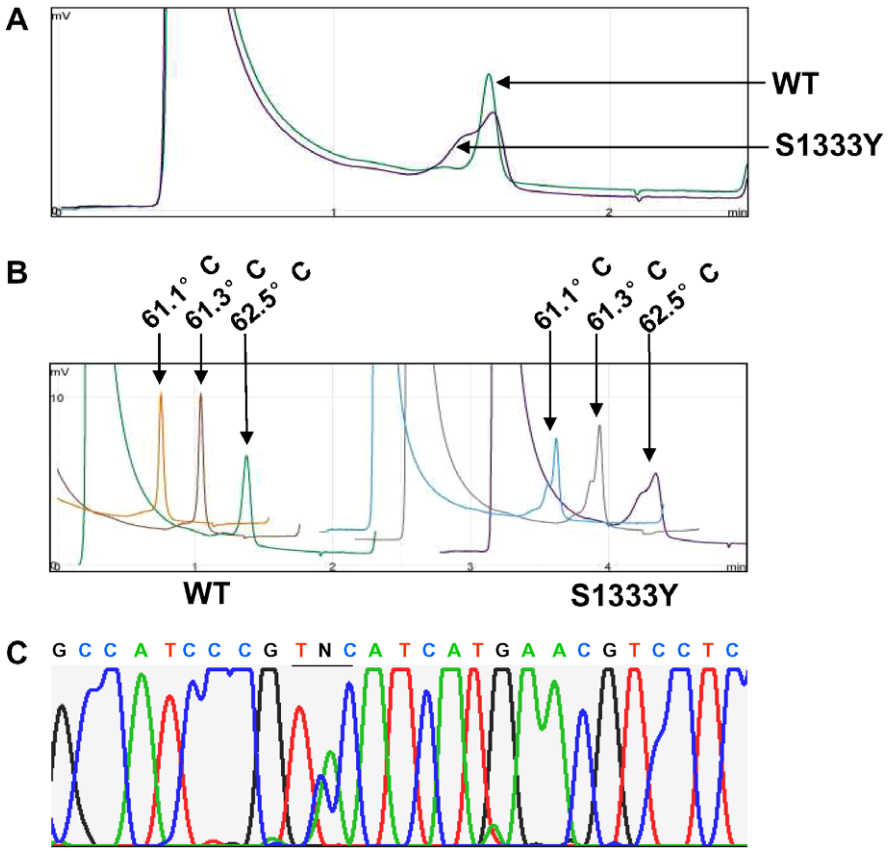

Fig. 1. Molecular identification of S1333Y. (A) DHPLC elution profiles of S1333Y identified in exon 23 of *SCN5A* at 62.5 °C. (B) DHPLC elution profile of S1333Y identified in exon 23 of *SCN5A* at 61.1, 61.3, and 62.5 °C. (C) Sequencing analysis showing a C-to-A substitution at position 3998 in exon 23, leading to a serine (S)-to-tyrosine (T) substitution at residue 1333.

responsible for the sudden death event in the patient. The sequencing analysis revealed a heterozygous C-to-A base change at position 3998 in exon 23 that resulted in a serine (S)-to-tyrosine (Y) substitution at residue 1333 (Fig. 1C). The mutation was in the S4–S5 linker in domain III, which plays a major role in fast inactivation of the Na^+ channel. This amino acid is highly conserved in the Na^+ channels of many species.

3.2. Biophysical characteristics of $Na_v1.5$/S1333Y

Whole-cell Na^+ currents were elicited by depolarizing steps from −100 to +50 mV with a holding potential of −140 mV (Fig. 2A). Current amplitudes were normalized to cellular membrane capacitance to generate current–voltage (*I–V*) curves in the form of current densities. Using the same data and graphically determined reversal potentials, the Na^+ conductance for the various voltages was calculated from the equation $G = I/(V - E_{rev})$, where I is the peak Na^+ current at a given voltage V and E_{rev}, the equilibrium potential extrapolated from the graph. *I–V* and conductance–voltage (*G–V*) curves were obtained for S1333Y and WT. The S1333Y mutant and WT channels had similar current densities, suggesting that they were expressed to the same extent on the cell membrane (Fig. 2B). The potential of the maximum peak current amplitude of the S1333Y channel was more negative than

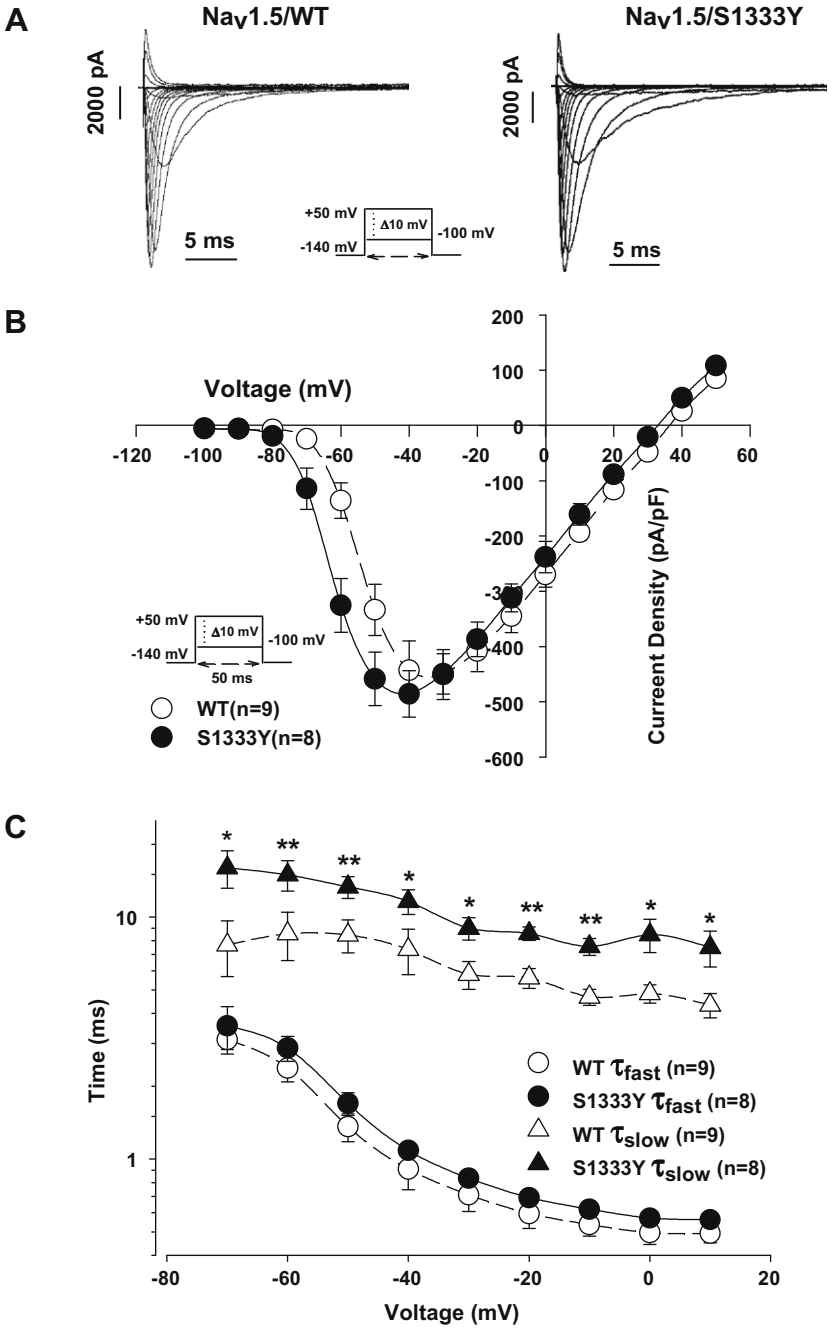

Fig. 2. Analysis of whole-cell currents recorded from tsA201 cells expressing WT and S1333Y. (A) I_{Na} from WT (left) and S1333Y (right) were elicited by depolarizing pulses from −100 mV to +50 mV in 10 mV increment for each step. (B) Current–voltage relationship of WT (○, $n = 9$) and S1333Y (●, $n = 8$). The current amplitude was normalized to the membrane capacitance. (C) The voltage-dependent time constants of inactivation in WT (○ for τ_{fast}, $n = 9$ and △ for τ_{slow}, $n = 9$) and S1333Y (● for τ_{fast}, $n = 8$ and ▲ for τ_{slow}, $n = 8$). Currents were fitted to a two-exponential function, obtaining the corresponding time constants τ_{fast} and τ_{slow} ($^*P < 0.05$ and $^{**}P < 0.01$).

that of the WT channel (Fig. 2B), which may be due to the coupled alteration of steady-state activation and inactivation. To analyze the effect of the S1333Y mutation on fast inactivation kinetics, the time constant τ was measured by fitting the decay of the whole-cell current elicited at each potential with the following double-exponential function: $I = I_{resid} + A_{fast} \times \exp(-(t-k)/\tau_{fast}) + A_{slow} \times \exp(-(t-k)/\tau_{slow})$, where I is the current density, I_{resid} the steady-state asymptotic residue, A_{fast} and A_{slow} are the percentages of channels inactivating with time constants τ_{fast} and τ_{slow}, and k is the time shift. Depolarizing steps from 2 to 50 ms were tested to ensure full current decay and the best fit. The S1333Y channel had a significantly longer time constant for the slow component than the WT channel over the entire voltage range from −70 mV to +10 mV (Fig. 2C). The most significant difference was at −20 mV, where the time constant τ_{slow} was 8.56 ± 0.54 ms (n = 8) for S1333Y and 4.67 ± 0.36 ms (n = 9) for WT. The slower decay of τ_{slow} indicated a decelerated inactivation of open channels. G–V curves were fitted to a standard Boltzmann distribution $G(V)/G_{max} = 1/(1 + \exp(-(V - V_{1/2})/k))$, where $G(V)$ is the conductance at a given voltage V and G_{max} is the maximum conductance. The midpoint of activation voltage ($V_{1/2}$) and the slope factor (k) were determined from the fit. The steady-state activation of the S1333Y mutation was negatively shifted by 8 mV, with no difference in the slope factor (Fig. 3A, and values in Table 1).

Voltage-dependent steady-state inactivation was measured by applying 500 ms pre-pulses ranging from −140 to −30 mV, followed by a 20 ms test pulse at −30 mV. The test pulse current amplitude was normalized to the maximum current recorded during the pre-pulse and plotted versus the pre-pulse voltage to obtain the voltage-dependent inactivation curve, which was fitted to a standard Boltzmann distribution function $I(V)/I_{max} = 1/(1 + \exp((V - V_{1/2})/k))$, where $I(V)/I_{max}$ is the current ratio and V, the pre-pulse voltage. During steady-state inactivation, a + 7 mV shift for S1333Y was observed, but the slope factor was not significantly affected (Fig. 3A). $V_{1/2}$ and k were generated by fitting each data set with the standard Boltzmann function (see Table 1 for values).

Steady-state activation and inactivation shifts appeared to increase the window current for S1333Y, which is generated by the overlap between these two fitting curves (Fig. 3B and C). The window current in LQT3 is associated with steady-state Na^+ channels reopening. S1333Y (Fig. 3C) significantly enhanced area of the window current compared to WT (Fig. 3B).

During slow inactivation, some voltage-gated Na^+ channels become non-conducting following prolonged membrane depolarization. The course of slow inactivation was assessed using a two-pulse protocol with an initial conditioning pre-pulse and a final

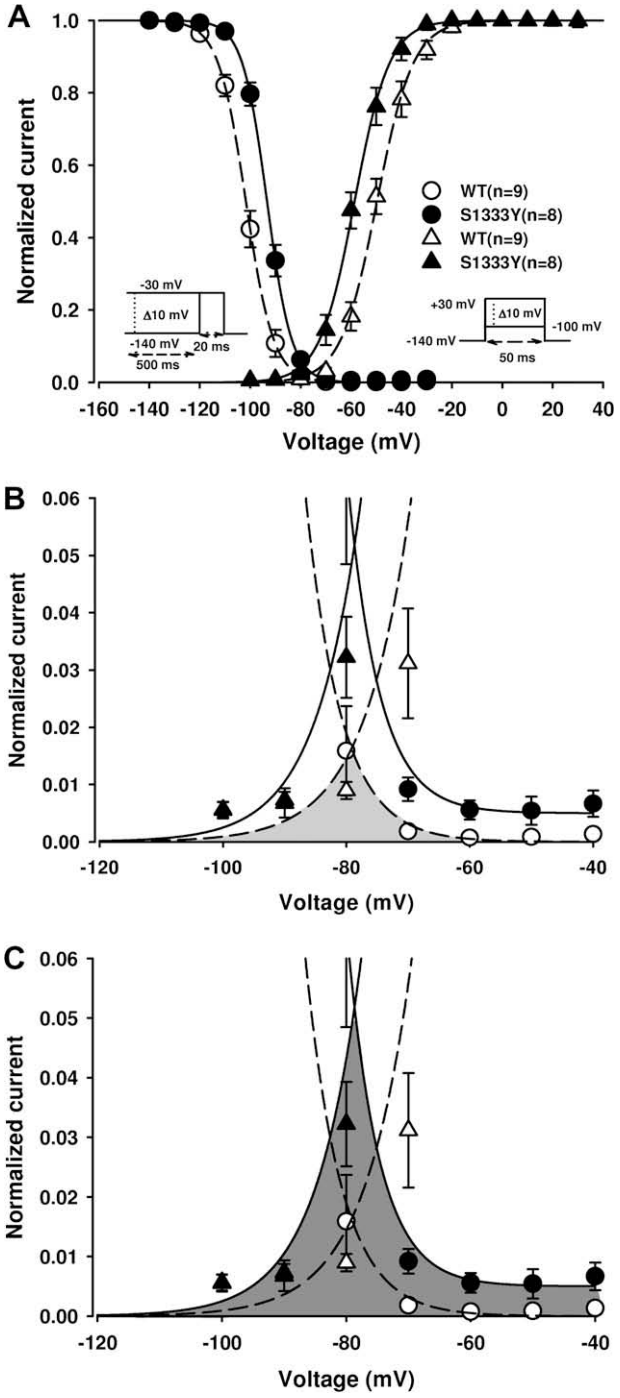

Fig. 3. The gating properties of steady-state activation and inactivation, and window currents. (A) Voltage-dependence of steady-state activation and inactivation in WT (△ for activation, n = 9 and ○ for inactivation, n = 9) and S1333Y (▲ for activation, n = 8 and ● for inactivation, n = 8). The activated and inactivated currents were generated from the protocols as inset, and their resulting data were fitted to a standard Boltzmann distribution. (B) The enlarged portion of overlap area (light grey) between activation and inactivation for WT. The shaded area represents the window region. (C) The enlarged part of overlap area (dark grey) between activation and inactivation for S1333Y. The shaded area was significantly enhanced than that of WT.

Table 1
Biophysical properties of $Na_v1.5$/WT and $Na_v1.5$/S1333Y.

	$Na_v1.5$/WT	$Na_v1.5$/S1333Y
Steady-state activation		
$V_{1/2}$ (mV)	−50.34 ± 2.06 (n = 9)	−58.88 ± 1.25* (n = 8)
K (mV)	−6.38 ± 0.27 (n = 9)	−6.13 ± 0.34 (n = 8)
Steady-state inactivation		
$V_{1/2}$ (mV)	−100.47 ± 1.34 (n = 9)	−93.46 ± 0.66** (n = 8)
K (mV)	4.91 ± 0.19 (n = 9)	4.91 ± 0.21 (n = 8)
Slow inactivation		
τ (ms)	327.78 ± 37.10 (n = 8)	306.96 ± 22.87 (n = 9)
Recovery from slow inactivation		
τ_{fast} (ms)	16.49 ± 4.73 (n = 7)	4.08 ± 0.60** (n = 7)
τ_{slow} (ms)	251.81 ± 60.79 (n = 7)	104.41 ± 27.06* (n = 7)
A_{fast}	91.7 ± 0.82% (n = 7)	94.33 ± 0.72% (n = 7)
A_{slow}	8.3 ± 0.82% (n = 7)	5.67 ± 0.72% (n = 7)
Closed-state inactivation		
−110 mV		
τ (ms)	89.54 ± 10.76 (n = 9)	60.28 ± 4.11* (n = 9)
−100 mV		
τ (ms)	109.51 ± 14.12 (n = 9)	65.82 ± 5.33** (n = 10)

$V_{1/2}$ = midpoint for activation or inactivation; K_v = slow factor for activation or inactivation; τ = time constant; and A = fraction of recovery component.
* $P < 0.05$.
** $P < 0.01$.

test pulse. A −30 mV pre-pulse was applied at intervals varying from 2 to 1000 ms, followed by a step to −140 mV for 20 ms to allow the channels to recover from fast inactivation. The −30 mV test pulse was applied for 40 ms to estimate the fraction of channels available for activation. The fraction was obtained by dividing the current amplitude during the test pulse by the current amplitude during the pre-pulse. Entry into slow inactivation followed a mono-exponential function $I = I_{resid} + A \times \exp(-t/\tau)$, where I is the current intensity, I_{resid} the asymptotic residual current, and A the current amplitude at time zero (see values in Table 1). As shown in Fig. 4A, there was no significant difference in the kinetics of entry into slow inactivation between the S1333Y mutation and WT. Recovery from slow inactivation was measured using a two-pulse protocol, where Na^+ channels were inactivated by a

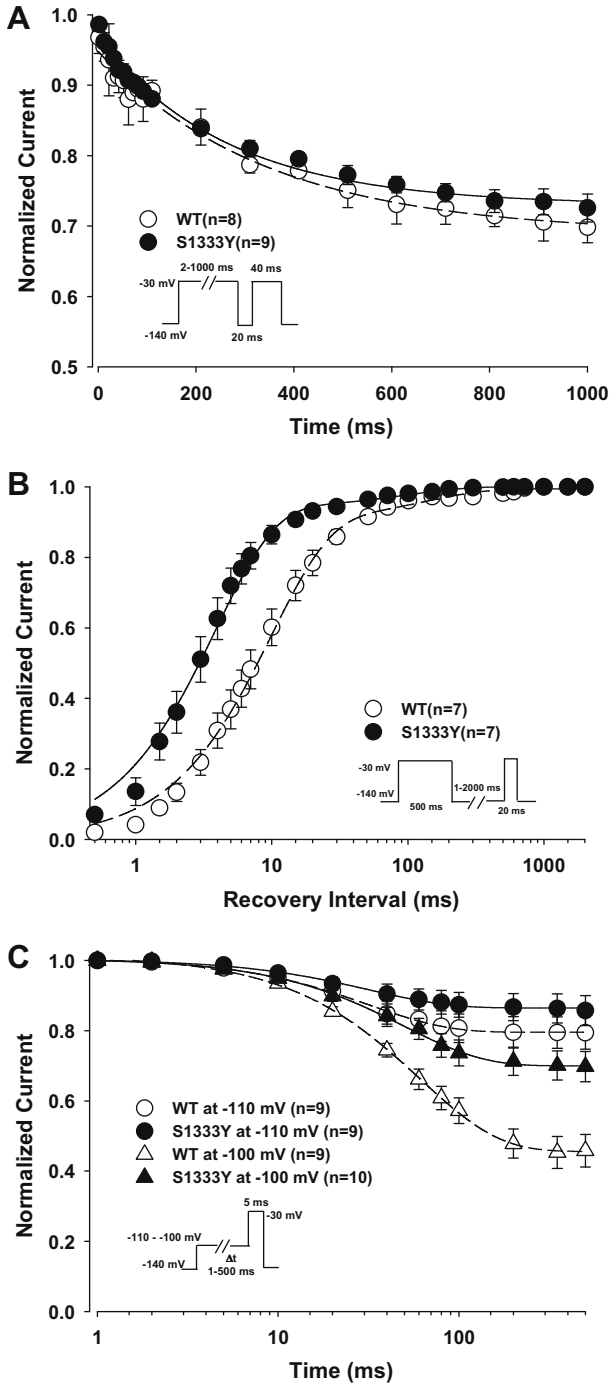

Fig. 4. The gating properties of slow inactivation, recovery from slow inactivation, and closed-state inactivation. (A) Slow inactivation in WT (○, $n = 8$) and S1333Y (●, $n = 9$). A two-pulse protocol as inset was used to generate the currents. The time constants (shown in Table 1) were obtained using a mono-exponential function. (B) Time courses of recovery from slow inactivation in WT (○, $n = 7$) and S1333Y (●, $n = 7$). A 500 ms conditioning pre-pulse was used to monitor recovery by a 20 ms test pulse after a variable recovery interval from 1 to 2000 ms (see protocol in inset). The time constants were obtained using a two-exponential function. (C) Closed-state inactivation in WT (○ for −110 mV, $n = 9$ and △ for −100 mV, $n = 9$) and S1333Y (● for −110 mV, $n = 9$ and ▲ for −100 mV, $n = 10$). The protocol in inset elicited the currents, which were fitted to a mono-exponential function.

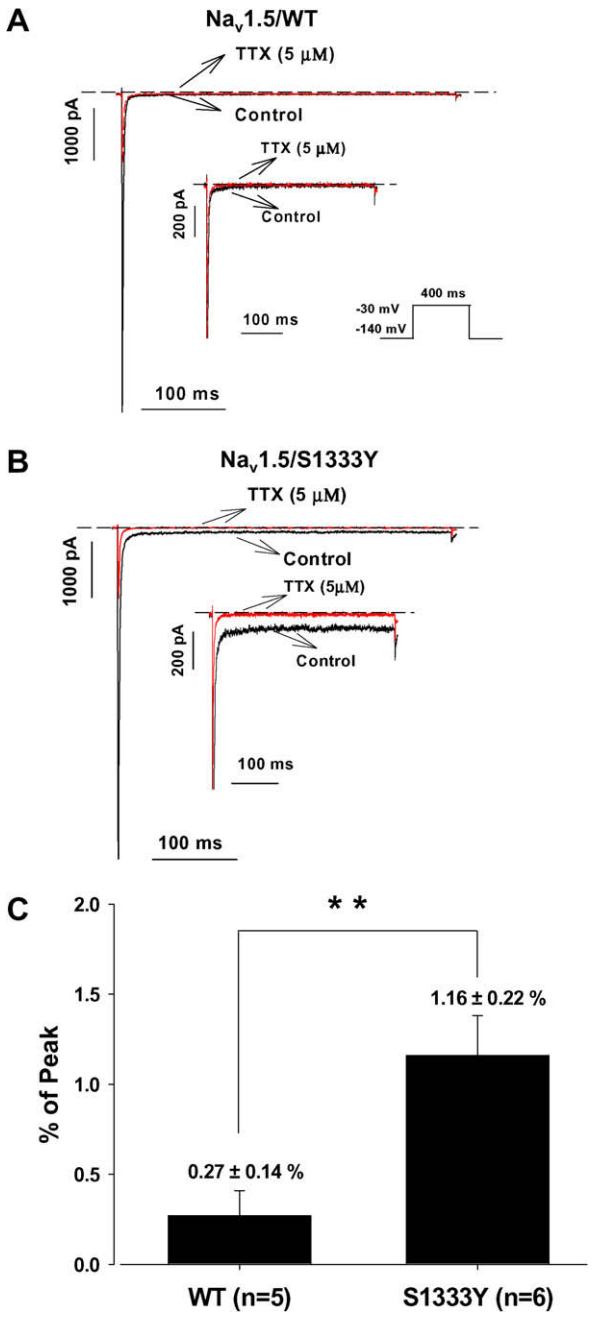

Fig. 5. Effect of TTX on the persistent sodium current in WT and S1333Y. The persistent sodium current was generated from a holding potential of +140 mV to −30 mV over 400 ms (see protocol in inset). The dashed line represents zero current. (A) Effect of adding 5 μM TTX to WT for 10 min. (B) Effect of adding 5 μM TTX to S1333Y for 10 min. The persistent sodium current was blocked by TTX. (C) The histogram of the persistent sodium current. The persistent sodium current accounted for 0.27 ± 0.14% of the peak current amplitude for WT ($n = 5$) and 1.16 ± 0.22% for S1333Y ($n = 6$) at −30 mV ($^{**}P < 0.01$).

−30 mV conditioning pulse for 500 ms, followed by a −30 mV test pulse after a recovery interval varying from 1 to 2000 ms. The peak current in response to the test pulse was normalized to the maximum peak current in response to the conditioning pulse. The normalized current was plotted against the recovery time interval. The resulting curve was fitted to a double-exponential function to obtain the following fast and slow components of recovery from slow inactivation: $I_{Na} = A_f \times (1 - \exp[-t/\tau_f]) + A_s \times (1 - \exp[-t/\tau_s])$, where t is the recovery time interval, τ_f and τ_f, the time constants of the fast and slow components, and A_f and A_s, the fractions of the fast and slow components (see values in Table 1). The results shown in Fig. 4B indicate that S1333Y recovered more rapidly from slow inactivation than WT.

The positive shift of the steady-state inactivation may be the result of fewer channels entering into closed-state inactivation (Fig. 4C). Closed-state inactivation primarily affects the availability of channels at voltages near the resting membrane potential, thus controlling the Na^+ current amplitude of the action potential. Using a double-pulse protocol, cells were pre-pulsed to −110 and −100 mV for periods ranging from 1 to 500 ms, and then stepped to −30 mV to determine the availability of I_{Na} during the pre-pulse. The time course was fitted with the following mono-exponential equation: $I = I_{resid} + A \times \exp(-t/\tau)$ (see values in Table 1).

Whole-cell Na^+ currents recorded in tsA201 cells expressing the WT *SCN5A* gene can exhibit a small persistent component whose magnitude depends on the recording conditions. The increased persistent Na^+ current in LQT3 mutants is a major factor in the prolongation of the QT interval. To study the contribution of the persistent current at steady-state, we measured the current using a 400 ms depolarization pulse. The persistent current was barely detectable in cells expressing WT channels (I_{per}/I_{peak} = 0.27 ± 0.14%, n = 5), while there was a significant increase in the persistent current in cells expressing the S1333Y mutation (I_{per}/I_{peak} = 1.16 ± 0.22%, n = 6) (Fig. 5C). Class I B Na^+ channel blockers (e.g., lidocaine) were reported to normalize prolonged QTc in LQT3 patients [15]. We therefore investigated the effect of lidocaine on the persistent inward Na^+ current of the S1333Y mutation. The persistent currents in WT and S1333Y were both blocked by 5 μM tetrodotoxin (TTX) (Fig. 5A and B) and 200 μM lidocaine (Fig. 6A and B), respectively.

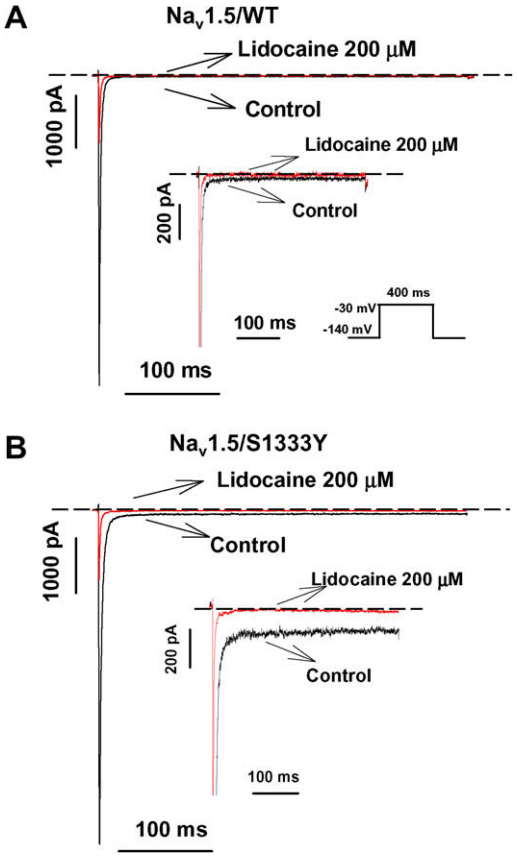

Fig. 6. Effect of lidocaine on the persistent sodium current in WT and S1333Y. The persistent sodium current was generated from a holding potential of +140 mV to −30 mV for 400 ms (see protocol as inset). The dashed line represents zero current. (A) Effect on WT of an 8-min treatment with 200 μM lidocaine on WT. (B) Effect on S1333Y of an 8-min treatment with 200 μM lidocaine. The persistent sodium current was blocked by lidocaine.

4. Discussion

In the present study, we biophysically characterized a new *SCN5A* mutation (S1333Y) in an infant who had died of SIDS. The mutation was located in the S4–S5 linker of domain III, which is often associated with inactivation changes in voltage-dependent Na^+ channels. The electrophysiological studies showed persistent Na^+ inward currents accompanied by a −8 mV shift in activation, and a +7 mV shift in inactivation. The window current was therefore enhanced by the shifts of activation and inactivation. The slow component of the fast activation of macroscopic currents of the mutation was slower than that of the WT. The serine at position 1333 is highly conserved, suggesting that this residue may play an important role in the channel gating.

Some inherited arrhythmic disorders (e.g., Brugada syndrome (BrS) and LQTS) appear to be associated with SIDS because they may explain the increased likelihood of sudden death when a trigger event occurs. Since the gating properties of BrS mutations are characterized by a loss of the Na^+ channel function, the present case is unlikely to be related to BrS.

The S1333Y mutation caused a serine-to-tyrosine substitution in the S4–S5 linker of domain III, which is near the proposed docking site of the inactivation particle. This mutation caused similar alterations in activation, fast inactivation, and kinetics of fast inactivation. Many LQT3 mutations have a persistent Na^+ current along with shortened fast inactivation time constants. However, R1623Q showed a slower rate of current decay that is in agreement with our results [16]. Reduced closed-state inactivation is consistent with the positive shift of inactivation. The rate of recovery from inactivation was also faster, which is in agreement with the findings reported for LQT3 mutations (ΔKPQ, R1644H, and E1784K) [14,17,18]. Faster recovery may increase the channel availability at the resting membrane potential of the ventricular cells. The shifts of activation and inactivation of the mutant enhanced the window current and an action potential could be triggered in this narrow region, The enhanced window currents can increase the risk of fatal ventricular arrhythmias especially when they coexist with persistent inward Na^+ currents. The A1330P *SCN5A* mutation, which also causes SIDS, is located near the site of the S1333Y mutation. A1330P causes a gain of Na^+ channel function by significantly increasing the window current. Interestingly, this mutation does not induce a persistent Na^+ current [7].

Mutations in the Na^+ channel associated with LQT3 usually result in a persistent Na^+ current flowing during the plateau phase of the cardiac action potential. At least five LQT3 mutations (S941N, A1330P, S1103Y, R1826H, and A997S) have been associated with SIDS [6–9]. Of these, two (R1826H and A997S) have a persistent inward Na^+ current. Moreover, in studies on relationships between cardiac polymorphisms and SIDS, a persistent Na^+ current was found in five of eight variants [19]. Such a persistent current may cause slower inactivation, resulting in prolonged

repolarization and thus a long QT interval. In the present study, the S1333Y mutation caused a persistent current that accounted for 1.16 ± 0.22% of the current amplitude. While there are no documented clinic findings to support the diagnosis of LQTS, we suspect that fatal ventricular arrhythmia may be triggered by an event such as the prone position during sleep.

We also found that the persistent current induced by S1333Y was sensitive to lidocaine. This suggests that the prolonged QT interval could be normalized by class I B Na^+ channel blockers. The mechanism of blocking the persistent current may be acted by lidocaine stabilizing inactivation, and thereby reducing the probability of dispersed and bursting activities in LQT3 mutant channels [20].

In the case presented here, sudden death occurred 25 days after delivery, and resuscitatory efforts were not possible given that SIDS happened too quickly. To prevent the sudden death event, a more effective way would be to diagnose the condition soon after delivery using the ECG that is faster and less expensive to perform. For those with a family history of SIDS and bradycardia, genetic analyses are recommended when the QTc exceeds 440 ms [8,21].

Acknowledgements

We would like to thank Valérie Pouliot for her technical assistance. This study was supported by a funding from the Heart and Stroke Foundation of Québec (HSFQ) and a grant from the Canadian Institutes of Health Research. M. Chahine is a J.C. Edwards Foundation Senior Investigator.

References

[1] Dwyer, T., Ponsonby, A.L., Newman, N.M. and Gibbons, L.E. (1991) Prospective cohort study of prone sleeping position and sudden infant death syndrome. Lancet 337, 1244–1247.
[2] Vege, A. and Ole, R.T. (2004) Sudden infant death syndrome, infection and inflammatory responses. FEMS Immunol. Med. Microbiol. 42, 3–10.
[3] Hunt, C.E. and Hauck, F.R. (2006) Sudden infant death syndrome. CMAJ 174, 1861–1869.
[4] Opdal, S.H. and Rognum, T.O. (2004) The sudden infant death syndrome gene: does it exist? Pediatrics 114, e506–e512.
[5] Arnestad, M., Crotti, L., Rognum, T.O., Insolia, R., Pedrazzini, M., Ferrandi, C., et al. (2007) Prevalence of long-QT syndrome gene variants in sudden infant death syndrome. Circulation 115, 361–367.
[6] Ackerman, M.J., Siu, B.L., Sturner, W.Q., Tester, D.J., Valdivia, C.R., Makielski, J.C., et al. (2001) Postmortem molecular analysis of *SCN5A* defects in sudden infant death syndrome. J. Am. Med. Assoc. 286, 2264–2269.
[7] Wedekind, H., Smits, J.P.P., Schulze-Bahr, E., Arnold, R., Veldkamp, M.W., Bajanowski, T., et al. (2001) De novo mutation in the *SCN5A* gene associated with early onset of sudden infant death. Circulation 104, 1158–1164.
[8] Schwartz, P.J., Priori, S.G., Dumaine, R., Napolitano, C., Antzelevitch, C., Stramba-Badiale, M., et al. (2000) A molecular link between the sudden infant death syndrome and the long-QT syndrome. New Engl. J. Med. 343, 262–267.
[9] Plant, L.D., Bowers, P.N., Liu, Q., Morgan, T., Zhang, T., State, M.W., et al. (2006) A common cardiac sodium channel variant associated with sudden infant death in African Americans, SCN5A S1103Y. J. Clin. Invest. 116, 430–435.
[10] Wang, D.W., Desai, R.R., Crotti, L., Arnestad, M., Insolia, R., Pedrazzini, M., et al. (2007) Cardiac sodium channel dysfunction in sudden infant death syndrome. Circulation 115, 368–376.
[11] Smith, M.R. and Goldin, A.L. (1997) Interaction between the sodium channel inactivation linker and domain III S4–S5. Biophys J. 73, 1885–1895.
[12] Millat, G., Chevalier, P., Restier-Miron, L., Da Costa, A., Bouvagnet, P., Kugener, B., et al. (2006) Spectrum of pathogenic mutations and associated polymorphisms in a cohort of 44 unrelated patients with long QT syndrome. Clin. Genet. 70, 214–227.
[13] Wang, Q., Li, Z., Shen, J. and Keating, M.T. (1996) Genomic organization of the human *SCN5A* gene encoding the cardiac sodium channel. Genomics 34, 9–16.
[14] Deschênes, I., Baroudi, G., Berthet, M., Barde, I., Chalvidan, T., Denjoy, I., et al. (2000) Electrophysiological characterization of SCN5A mutations causing long QT (E1784K) and Brugada (R1512W and R1432G) syndromes. Cardiovasc. Res. 46, 55–65.
[15] Groenewegen, W.A., Bezzina, C.R., van Tintelen, J.P., Hoorntje, T.M., Mannens, M.M.A.M., Wilde, A.A.M., et al. (2003) A novel LQT3 mutation implicates the human cardiac sodium channel domain IVS6 in inactivation kinetics. Cardiovasc. Res. 57, 1072–1078.
[16] Kambouris, N.G., Nuss, H.B., Johns, D.C., Tomaselli, G.F., Marban, E. and Balser, J.R. (1998) Phenotypic characterization of a novel long-QT syndrome mutation (R1623Q) in the cardiac sodium channel. Circulation 97, 640–644.
[17] Dumaine, R., Wang, Q., Keating, M.T., Hartmann, H.A., Schwartz, P.J., Brown, A.M., et al. (1996) Multiple mechanisms of Na^+ channel-linked long-QT syndrome. Circ. Res. 78, 916–924.
[18] Chandra, R., Starmer, C.F. and Grant, A.O. (1998) Multiple effects of KPQ deletion mutation on gating of human cardiac Na^+ channels expressed in mammalian cells. Am. J. Physiol. 274, H1643–H1654.
[19] Wang, D.W., Desai, R.R., Crotti, L., Arnestad, M., Insolia, R., Pedrazzini, M., et al. (2007) Cardiac sodium channel dysfunction in sudden infant death syndrome. Circulation 115, 368–376.
[20] Dumaine, R. and Kirsch, G.E. (1998) Mechanism of lidocaine block of late current in long Q-T mutant Na^+ channels. Am. J. Physiol. 274, H477–H487.
[21] Schwartz, P.J., Stramba-Badiale, M., Segantini, A., Austoni, P., Bosi, G., Giorgetti, R., et al. (1998) Prolongation of the QT interval and the sudden infant death syndrome. New Engl. J. Med. 338, 1709–1714.